Tafreshi, S.N. Moghaddas and Khalaj, Omid and Dawson, Andrew (2014) Repeated loading of soil containing granulated rubber and multiple geocell layers. Geotextiles and Geomembranes, 42 (1). pp. 25-38. ISSN 0266-1144

Repeated loading of soil containing granulated rubber and multiple geocell layers

S.N. Moghaddas Tafreshi[1,*] (Corresponding Author), O. Khalaj [2], A.R. Dawson[3]

[1,*]***Corresponding Author**, Associate Professor, Department of Civil Engineering, K.N. Toosi University of Technology,* Valiasr St., Mirdamad Cr., *Tehran, Iran. Tel: +982188779473; Fax: +982188779476; E-mail address: nas_moghaddas@kntu.ac.ir*

[2]*Department of Civil Engineering, PhD Candidate, K.N. Toosi University of Technology, Tehran, Iran. Tel: +982188779473; Fax: +982188779476; Email: o_khalaj@yahoo.com*

[3]*Associate Professor, Nottingham Transportation Engineering Centre, University of Nottingham, Nottingham, UK. Tel: +44 115 951 3902; fax: +44 115 951 3909. E-mail address: andrew.dawson@nottingham.ac.uk*

ABSTRACT: Sandy soil/aggregate, such as might be required in a pavement foundation over a soft area, was treated by the addition of one or more geocell layers and granulated rubber. It was then subjected to cyclic loading by a 300 mm diameter plate simulative of vehicle passes. After an initial study (that established both the optimum depth of the uppermost geocell layer and of the geocell inter-layer spacing should be 0.2 times plate diameter), repeated loading was applied to installations in which the number of geocell layers and the presence or absence of shredded rubber layers in the backfill was changed. The results of the testing reveal the ability of the composite geocell-rubber-soil systems to 'shakedown' to a fully resilient behavior after a period of plastic deformation except when there is little or no reinforcement and the applied repeated stresses are large. When shakedown response is observed, then both the accumulated plastic deformation prior to a steady-state response being obtained and the resilient deformations thereafter are reduced. Efficiency of reinforcement is shown to decrease with number of reinforcement layers for all applied stress levels and number of cycles of applied loading. The use of granulated rubber layers are shown to reduce the plastic deformations and to increase the resilient displacements compared to the comparable non-rubber construction. By optimal use of geocells and granulated rubber, deformations can be reduced by 60-70% compared with the unreinforced case while stresses in the foundation soil are spread much more effectively. On the basis of the study, the concept of combining several geocell layers with shredded rubber reinforcement is recommended for larger scale trials and for economic study.

***Keywords**:* Pavement foundation, Repeated loading; Multiple geocell layers; Rubber-soil mixture layer; Residual and resilient deformations.

1. Introduction

Geosynthetic-reinforced soil offers economy, ease of installation, performance and reliability in many areas of geotechnical engineering e.g., construction of footings over soft soil, stable embankments, slope and earth stabilization, road construction layers, and pavement system (e.g., Hufenus et al., 2006; Dash et al., 2007; Bathurst et al., 2009; Madhavi Latha and Somwanshi, 2009; Zhang et al., 2010; Pokharel et al., 2010; Moghaddas Tafreshi and Dawson, 2012; Boushehrian et al., 2011; Lambert et al., 2011; Koerner, 2012. Yang et al. 2012; Thakur et al., 2012; Tavakoli et al., 2012; Leshchinsky and Ling, 2013; Tanyu et al., 2013, Chen et al., 2013).

Boushehrian et al. (2011) investigated the cyclic behavior of three-dimensional (a grid-anchor reinforcement system) reinforced sand by conducting a series of field tests. They reported the benefit of the three-dimensional reinforced system over the conventional geomesh system in reducing the settlements of foundations rested on sand bed. Thakur et al. (2012) investigated the performance of single geocell-reinforced recycled asphalt pavement (RAP) bases, reporting that the geocell-reinforced RAP bases had much smaller permanent deformations and smaller vertical stresses than unreinforced base, at the interface between base and subgrade.

Overall, geosynthetic inclusions would be most effective if used in the zone significantly stressed by the loading surface (e.g., footing or tire wheel) – which may be over a depth of 1 or 2 width/diameters beneath the footing/tire wheel – i.e. over a depth of approximately 0.6 – 2 m for typical footing widths and over a depth of 0.3 – 0.6 m for typical tire wheel widths. Since, the heights of commercially produced geocells are usually standard and manufacturers of geocell produce them at heights less than 200 mm (available cell depths produced by two key manufacturers in Europe and the USA), using a 0.6 to 2 m single thick layer of geocell beneath the footing and tire wheel is not possible for field construction. Even if it were, such a thick geocell layer would likely make compaction of cell-fill extremely difficult (Thakur et al. (2012) and as has been demonstrated by the authors' observation and the result of tests not reported here), consequently decreasing the performance of a thick single layer of geocell. Hence, if such a thickness of soil were to be reinforced by geocells, it would require, say, 3 or 4 layers with thickness ≤ 200 mm.

In the last decades, the volume of used tire rubbers in the world have been significantly increased due to the developing industry and growing population (WRAP, 2007; RMA, 2007; RRI, 2009) and their disposals have, therefore, become a major environmental problem worldwide. Large numbers of scrap tires are either dumped in landfills or stockpiled across the landscape in huge volume (Cetin et al., 2006; Chiu, 2008). It makes them harder and more expensive to dispose of safely without threatening human health and environment. For instance, stockpiled waste tires are flammable, prone to fires with toxic fumes and may then cause a major health hazard for both human beings and animals (Attom, 2006).

Hence, to consider the environmental concerns and a greater willingness, the use of waste tires in the form of strips, chips, and granules, are now considered as construction materials (Tanchaisawat et al., 2010; Lovisa et al., 2010; Tavakoli et al., 2012; Moghaddas Tafreshi et al., 2012; Edincliler and Cagatay, 2013). When the chipped, shredded and granulated tire rubbers are mixed with soil (or the strips of tire used as reinforcement), the mixture can behave as a composite material. It becomes a form of reinforced soil, similar to geosynthetic-reinforced soil, that can be advantageously employed to increase soil strength (Yoon et al., 2008; Tavakoli et al., 2012). The cyclic load response of rubber-soil mixtures (e.g. as identified by Bosscher et al., 1997; Feng and Sutter 2000; Edincliler et al., 2004; Prasad and Prasada Raju, 2009) has shown the material's potential as a composite material, particularly in applications in roads, highways, and embankments. Bosscher et al. (1997) used tire-chips in soil to form a laboratory model embankment which was then subjected to simulated, repeated traffic loads. Less surface plastic displacement was reported when the tire-chips were covered by a relatively thick soil-only layer than when the tire-chips were placed in the whole of the fill. The soil cap over the tire-chips not only reduces the on-going settlement, but also prevents tire shreds from possible ignition.

On the basis of this review, the present authors considered that there could be potential for combining these two techniques (combining the layers of geocell with rubber-soil mixture layers) to improve the strength and to reduce the deformation within pavement foundations and, specifically, weak locations in these layers (e.g. trench reinstatements).

However, the economic evaluation of a complex rubber-soil mixture together with multiple geocell layers would be an essential consideration of any practical project. So far this has not been investigated in any recent research and, regrettably, space doesn't allow this aspect to be investigated here. In Europe at least, the ban on land-filling of old tires makes, in principle, economic sense of the beneficial reuse of rubber and the economic incentive to provide safe, post-consumer uses of rubber may be sufficient to partially finance the geocell reinforcement. This possibility should be studied further. With the evident benefit of using multiple geotextile or geogrid layers (e.g. Sitharam and Sireesh, 2005), the use of multiple geocell layers could be effective. Although it might be anticipated that more geocell layers in a foundation bed reduce the deformations, but there is much detail of the use of multiple geocell layers with and without rubber-soil combinations under repeatedly applied loads which has not been investigated by researchers. Consequently, this paper seeks to address the concept of the reinforcing benefit of the added rubber in association with the geocell layers which would have application, potentially, to pavement foundation (or machine support) systems.

2. Objectives

The overall goal was to demonstrate the benefits of introducing multi-layered geocell and combining this with rubber reinforcement to address weak spots in pavement foundations (e.g. at trench reinstatements). Cyclic loading conditions were selected as these are of particular concern for pavement (or machine foundation) problems where localized soil reinforcement might be appropriate. Thus a total of 21 independent cyclic plate load tests (plus 13 repeated tests) of a pavement foundation supported on unreinforced soil or soil reinforced with geocell and rubber were performed in a test pit measuring 2000×2000 mm in plane and 700 mm in depth using a 300 mm diameter rigid steel plate. Testing was arranged so as to determine the parameters controlling best usage. The specific aims were to study (The numbers in parentheses indicated the relevant results section):

- the optimal depth of the top geocell layer (6.1),
- the optimal vertical spacing between successive layers of geocell (6.2),
- the effects of the number of geocell layers on residual and resilient settlements (6.3.1 and 6.3.2),
- the effects of the geocell layers on the stress profile with depth (6.3.3), and
- the additional effect of the rubber-soil mixture layers on the residual and resilient settlements (6.4.1 and 6.4.2) and on the stress profile (6.4.3).

3. Test Materials

3.1. Soil materials

The backfill soil selected for the testing program was sourced from a local quarry and satisfies the criteria and limitations recommended in ASTM D 2940-09. It was a sandy soil passing through the 38 mm sieve (see Fig. 1) with a specific gravity, G_s, of 2.65. According to the Unified Soil Classification System (ASTM D 2487-11), the sand is classified as well graded sand with letter symbol *SW*. According to the modified proctor compaction tests (ASTM D 1557-12), the maximum dry density was about 20.62 kN/m^3, which corresponds to an optimum moisture content of 5.7%. The angle of internal friction (φ) of sand obtained through triaxial compression tests at a wet density of 19.58 kN/m^3 (corresponding to 90% of maximum dry density) was 40.5°. This soil was used to fill the cells of the polymeric reinforcement and, when required, mixed with rubber for use between the geocell layers.

The natural ground soil, at the bottom and four side walls of the test pit, has a maximum particle size of about 20 mm and a specific gravity, G_s, of 2.62. This soil is classified as SP in the Unified Soil Classification System (ASTM D 2487-11). The wet density and the natural moisture content of this soil were measured as 17.9 kN/m^3 (it corresponds to 90% of maximum dry density of 20.25 kN/m^3) and 9%, respectively. The angle of internal friction (φ) of the natural soil at a wet density of 17.9 kN/m^3 was 32.5°. The dimensions of the excavated test pit relative to the loading plate diameter are sufficient to minimize boundary effects. The natural ground soils were selected so as not be excessively soft and weak. In this way the assessment of reinforcing benefit from the installations investigated might be conservative. However, the use of a softer subgrade might show the benefits of rubber-soil with geocells to be even better.

3.2. Geocell reinforcement

A geocell was chosen that had been fabricated from a non-woven geotextile by thermo-welding so as to form a "honeycomb" arrangement (Fig. 2). When filled with soil this geocell provides confinement chambers for the soil, thereby developing frictional strength in the soil and shear resistance at the soil-geocell interfaces due to locally high passive earth pressure. The overall effect is to restrict lateral displacement of infill, to increase the bearing pressure, and to limit the subsidence of the foundation. Strong welds and parent material are required to ensure reliably high load-bearing capacity, otherwise rupture of the reinforced soil could result (Moghaddas Tafreshi and Dawson, 2012). According to the manufacturer, the strength and stiffness of the geocell joint is higher or similar to that of the geocell wall material (i.e. geotextile). The engineering properties of the geotextile from which geocell is formed and the geometry of the geocell, as listed by the manufacturer, are presented in Table 1. Geocell pocket size (*d=110 mm*), loading plate diameter (*D=300* mm) and height of geocell (H_g= *100* mm) were kept constant. However, the *d/D* ratio adopted may not the optimum value and a change in *d/D* might change the results. The effect of *d/D* could be investigated in future studies.

3.3. Rubber

The rubber used in the study comprised granulated particles with a specific gravity, G_s, of 1.17, between 2 mm and 25 mm sieve size, and a mean particle size of 14 mm. The rubber particles were clean and free of any steel and cord. Fig. 1 and Fig. 3 show, respectively, the grading and a photograph of this material. When required (see Section 5), to form the combined soil and rubber mixtures placed between the layers of geocell, the backfill soil and the rubber were carefully blended into the soil using a mixer, with manual intervention if necessary, so as to produce a reasonably uniform, non-segregated, rubber-soil mixture.

4. Full scale model test

To evaluate the performance improvement in the deformation and the stress profile of pavements supported by layers of geocell and by layers of rubber-soil mixture, and to provide realistic test conditions, a full scale model test of a standard plate load was conducted. The schematic cross-section of the test set-up of the foundation bed containing a model test pit trench, geocell-reinforcement layers, rubber-soil mixture layers, the loading plate model, loading system and data measurement system (dial gauges and soil pressure cells), the geometry of the test configurations, and location of three soil pressure cells, is shown in Fig. 4.

4.1. Test pit and instrumentation

All plate load tests were conducted in an outdoor test pit (see Acknowledgements). The test pit, measuring 2000 mm × 2000 mm in plan, and 700 mm in depth, was excavated in natural ground to construct the geocell layers, rubber-soil mixture layers and to install the pressure cell at specified depths. The load application system was an hydraulic jack imposed by a manually-operated pump and supported against a strong reaction beam spanning the width of the test pit. The steel rigid circular plate of 300 mm in diameter and 25 mm in thickness was placed on the surface at the center of the installation. An additional 10 mm thick rubber base was attached at the bottom of the loading plate to simulate the rubber tire contact with the ground surface. To measure the movement of the plate, throughout the tests, three linear dial gauges with an accuracy of 0.01% of full range (100 mm) were attached to a reference beam and their tips placed about 10 mm inwards from the edge of the plate. Also, to measure the vertical stress inside the foundation bed, it was instrumented with three full bridged, 50 mm diameter diaphragm-type soil pressure cells (SPC). These had an accuracy of 0.1% of full range of 1000 kPa according to the manufacturer. The top soil pressure cell (abbreviated to "T.SPC"), middle soil pressure cell ("M.SPC"), and bottom soil pressure cell ("B.SPC") are located at 190 mm, 350 mm, and 510 mm beneath the center of loading plate (Fig. 4). The instruments' output was recorded in mV and then converted to stress units using established calibrations for the sensors. To ensure an accurate reading, all of the devices were calibrated prior to each test series.

Since the pressure cells are located at the middle of soil layers or at the middle of the rubber-soil mixture layers (see Fig. 4), to simulate the real test condition and to obtain the calibrations for the pressure cells, a 300 mm-diameter and 200 mm-high cylinder container made of very soft textile was filled with the soil/soil-rubber mixture and each cell was placed, in turn, in the middle. The container was then placed in a compression machine and the cells were calibrated for different levels of cyclic applied pressure. A photograph of the test installation prior to testing, showing the reaction beam, load plate, hydraulic jack and three dial gauges is presented as Fig. 5.

4.2. Backfill compaction

In order to compact the layers of the foundation including unreinforced soil, geocell-reinforced layers and rubber-reinforced layers, a walk-behind vibrating plate compactor, 450 mm in width, was used. In all the tests, the compactor passed over the backfill at ten levels being 0, 60, 160, 220, 320, 380, 480, 540, 640, and 700 mm from the level of the base of the loading plate. To achieve the required density of soil that filled the geocell pockets (see Table 2), more passes of the compactor were needed compared to the unreinforced layer. Hence, the unreinforced layers, geocell reinforced layers and rubber soil mixture layers were compacted at an optimum moisture content of 5.7% with two, three and three passes, respectively so that the compactive effort, and consequently compaction energy, was kept the same for all passes of the compactor. To better assess the layers' compaction, three sand cone tests in accordance with ASTM D 1557-12 were conducted in some installations and after layer compaction, to measure the densities and moisture content of compacted soil layers, rubber-soil mixture layers and the density of the soil filled into the geocell pockets. The density values measured in the three cone tests revealed a close match with maximum differences in results of only a rather small 1-1.5%. The average measured (recovered) moisture content of the layers was between 5.2% and 5.7%. To prevent loss of moisture from the backfill during the load test, the exposed backfill was covered to a distance of 1.8 m from the circumference of the bearing plate with a waterproof paper. Table 2 shows the average measured dry densities (average of three sand cone tests) of unreinforced soil, the soil filled in geocell pockets, and rubber-soil mixture after compaction of each layers. Note the reduction in density as a consequence of compaction inside geocell pockets and due to the partial replacement of mineral by the less dense rubber particles and of the differing void ratios.

4.3. Loading system and simulated tire pressure

The loading arrangements were chosen to represent the tires of typical trucks on a pavement. While general traffic loading will not be applied to the geocell-aggregate layers but millions of times to overlying asphalt layers, such loading will be applied for a few traffic passages during construction and this will, likely, be the most demanding time for the reinforced foundation. In addition, AASHTO T 221-90 and ASTM D D1195-09 recommend application a few load cycles using repetitive static plate load tests of flexible pavement for use in evaluation and design of airport and highway pavements. It is this loading which was simulated in the work described here by distributing wheel loads over an equivalent circular area at the appropriate tire pressure (Brito et al., 2009).

Hence, in order to simulate the effect of wheel loading, unloading and reloading were imposed through the plate at a rate of 1.5 kPa per second. The maximum applied pressure was chosen to replicate that of a heavy vehicle half-axle with “Super-Single” tire, as used on a common heavy trailer (6 axles and a mean pressure 792 kPa) (Brito et al., 2009) and was divided into two stages being 400 and 800 kPa to simulate half and full traffic loadings. For each stage, fifteen loading and unloading cycles were applied. Preliminary repeated load tests (which are not reported in the paper) showed that (regardless of the number of geocell layers, number of rubber-soil mixture layers and the amplitude of applied load) with increase in the number of load cycles, the rate of change of loaded surface deformations reduces, so that their response has become, approximately, stable within fifteen load cycles. This implies that a large number of cyclic load applications were not essential.

Although, the rotating stress field applied by a wheel passage is rather different from the cyclic axial loading applied in these tests, yet Kim and Tutumluer (2005) showed that cyclic plate load tests can deliver useful results in the absence of moving wheel load test. Thus, any benefits of the geocell and rubber reinforcements arrangements discovered in the present study may be anticipated to under-estimate those that might be experienced under wheeled traffic. Therefore, this limitation in the present work isn't expected to be very influential on the outcomes.

5. Test program

Five test series for the unreinforced bed, the multi-layered geocell and the combined use of geocell reinforcement layers and rubber-soil mixtures reinforcement layers were conducted (see Table 3 for details). Test Series 1 provided reference, unreinforced, performance data. Test Series 2 and 3 were performed to obtain the optimum values of the depth of the first layer of geocell reinforcement beneath the loading plate (u), and the vertical spacing of the geocell layers (h). To investigate the effect of number of geocell layers on the deformation response of pavement, Test Series 4 was conducted by varying the number of geocell layers (N_g=1, 2, 3, 4), when the layers of geocell were placed at the optimum values of u/D and h/D (u/D=h/D=0.2) previously identified by Test Series 2 and 3.

To investigate the beneficial effect of combined use of geocell reinforcement layers and rubber-soil mixtures reinforcement layers on deformation of loading plate and on the stress profile with depth, Test Series 5 was conducted. In these tests equal numbers of layers of each type (i.e., N_g=N_{rs}=1; N_g=N_{rs}=2; N_g=N_{rs}=3 and N_g=N_{rs}=4) were used, where N_{rs} is the number of soil-rubber layers. In the Test Series 5, the soil layers between the geocell layers (with thickness of h) are substituted by mixed rubber-soil layers (with thickness of h_{rs}), so that h/D=h_{rs}/D=0.2. Granulated rubber was used at a mass replacement rate of 8% (a value based on the findings of the authors in earlier work (Moghaddas Tafreshi et al., 2013) which used static plate loading of a combined multi-layered geocell and rubber reinforced foundation to determine the optimum replacement proportion) in the middle of the rates of 6% and 10% recommended, respectively, by Prasad and Prasada Raju (2009) and Munnoli et al (2013).

The width of the both geocell and rubber-soil mixture layers (*b*) and the depth to the top of the first geocell layer below the footing (*u*) are expressed in non-dimensional form with respect to loading plate diameter (*D=300 mm*) as, *b/D* and *u/D*. In line with the findings of Dash et al., (2003), Yoon et al., (2008) and Thakur et al., (2012), the parameter *b/D* was held constant in all the tests at *b/D*=5. The variable parameter, *h*, is used to describe the vertical spacing between the bottom of the previous layer of geocell and the top of the next layer. It is expressed in non-dimensional form with respect to loading plate diameter (*D*) as *h/D*, whereas the height of geocell layers (H_g) is expressed in dimensional form (100 mm) and the height of the rubber-soil mixture layers (h_{rs}) is considered equal to *h* (the vertical spacing between the bottom of the previous layer of geocell and the top of the next layer).

In order to assess the utility of the apparatus, the accuracy of the measurements, the repeatability of the system, the reliability of the results and finally to verify the consistency of the test data, many of the tests described in Table 3 were repeated at least twice. The results obtained revealed a close match between results of the two or three trial tests with maximum differences in results of around 6-8%. This difference was considered to be small and is subsequently neglected. The consistency of the results demonstrates that the mixture of soil and rubber, the test procedure and technique adopted can produce repeatable tests within the bounds that may be expected from geotechnical and pavement testing apparatus.

6. Results and discussion

In this section, the results of cyclic plate load tests are presented along with a discussion highlighting the effects of the different parameters. The performance improvement of the reinforced bed is represented here by variations in the plate settlement and the distributed pressure at depth of the pavement foundation beds. Note that, in order to save time in Test Series 2 and 3, only one load cycle for each of the six cyclic pressures (150, 300, 400, 600, 700, and 800 kPa) was applied on the same section used for each installation with a particular u/D and h/D ratio. In Test Series 1, 4 and 5, fifteen cycles of loading and unloading at 400 and 800 kPa pressure were applied on the same section used in each test.

6.1. The optimum value of the depth of the first layer of geocell layer (u/D ratio)

Variation of residual plastic deformation of the loading plate (averaged from three dial gauges) as a function of the depth of the first layer of geocell reinforcement beneath the loading plate (*u/D* ratio) with a single layer of geocell reinforcement (N_g=1) at different amplitudes of cyclic load (=150, 300, 400, 600, 700, 800 kPa) is shown in Fig. 6 (Test Series 2). In these tests, only one cycle of load was applied at the surface of loading plate. This figure shows that the value of plastic deformation increases with increase in the applied cyclic pressure, irrespective of the *u/D* ratio. From this figure, it is found that the minimum value of plastic deformation was obtained at a *u/D* value of approximately 0.2, irrespective of amplitude of cyclic load. The figure shows the plastic deformation of the geocell reinforced bed initially decreases while the depth of placement increases from *u/D*=0 to *u/D*≈0.2, but that, thereafter, with increase in the *u/D* ratio, the value of plastic deformation increases again. The slight increase in performance improvement until *u/D*≈0.2 could be due to the surface soil layer, above the first geocell layer, acting as a cushion, preventing the direct contact of the loading plate base with the cell walls and distributing the applied pressure more uniformly over the cellular geocell. The other probable reason why a small cover thickness is desirable is that the confinement provided by the soil above the geocell layer helps to develop frictional resistance between the geocell and the soil. Similar findings, under monotonic loading have been reported by Sitharam and Sireesh (2005) and Yoon et al. (2008),

Likewise, as the value of *u/D* increases beyond 0.2 (toward 0.6), the top geocell layer moves out of the zone where it can most successfully interrupt the applied stress field and, hence, the plastic deformation increases. Finally, as expected, with increase in *u/D* ratio to about one, the geocell layer lies almost entirely outside of the significantly stressed zone under the loading plate so that the influence of reinforcement becomes negligible, and the overall response approaches that of an unreinforced pavement foundation.

Although the optimum *u/D* value might be a function of loading plate size, the height of geocell layers, the geocell pocket size, type of soil and the number of geocell layers, in the present study, in all the subsequent plate load tests, the geocell reinforcement was placed at *u/D*=0.2. Yoon et al. (2008), in their studies using a circular plate of diameter (*D*) 350 mm resting on sand reinforced with multiple layers of 'Tirecell' (made from treads of waste tires), reported a similar finding for a *u/D* ratio (*u/D*=0.2). Therefore, in the present study, use of *u/D* ratio of 0.2 appears defensible.

6.2. The optimum value of the vertical spacing of the geocell layers (h/D ratio)

Fig. 7 illustrates the variation of residual plastic deformation of loading surface with vertical spacing of the geocell layers (*h/D* ratio) for two layers of geocell (N_g=2) at different amplitudes of cyclic load (= 150, 300, 400, 600, 700, 800 kPa) - the results of Test Series 3. In these tests only one cycle of load was applied. From this figure, it can be seen that, regardless of the amplitude of cyclic load, the plastic deformation is minimized when the *h/D* ratio is approximately, 0.2. The reduction in plastic deformation at *h/D* of 0.2 may be attributed to the behavior of the soil layer between the first and the second layers of geocell. At small thicknesses it provides effective load spreading without deforming much laterally as it is confined by the geocell reinforcement above and below. However, if the reinforcing layers become too widely spaced, then the material between the geocell layers can be displaced, weakening the overall response. Yoon et al. (2008) in their studies using static plate loading test (see end of section 6.1, above) reported that the effective placement of 'Tirecell' reinforcement was best at a vertical spacing of reinforcement layers of 0.2 times the plate diameter. It is of interest to note that, in spite of differences between the present study and the studies of Yoon et al. (2008) in the footing size, the soil properties, type of 3D reinforcement, the geometric dimensions of the reinforcement, and the type of loading (they used the monotonic loading whereas this study also investigates unloading) the optimum values of *u/D* and *h/D* from the present study are consistent with those reported by Yoon et al. (2008).

In addition, it can be seen from Fig. 7 that the effect of geocell-reinforcement spacing is more significant at higher amplitudes of cyclic load, whereas for the low amplitude of cyclic load, the improvement in plastic deformation does not vary much with the variation in reinforcement spacing. It indicates that at low stress amplitude levels the second layer of geocell has hardly been strained by the load applied to the soil surface and, consequently, has little beneficial effect.

Likewise, Fig. 7 shows an increase in the plastic deformation, regardless of the amplitudes of cyclic load, with increasing *h/D* beyond the optimum value. It would be expected that, when the value of *h/D* reaches a thickness of 0.8-1 times the loading plate diameter, the second geocell layer would be, largely, outside of the zone of significant stress due to the surface loading, so that its influence on foundation bed behavior would become negligible and the behavior of a reinforced system with two layers of geocell would tend to that of a reinforced system supported by a single layer of geocell. The results of experimental studies conducted by

Chen et al. (2013) and Abu-Farsakh et al. (2008) indicated that the vertical spacing of planar reinforcement layers needs to be less than 0.5 times of footing width to prevent the failure between reinforcement layers from occurring.

Hence, in the present study, and in order to investigate the effect of multi-layered geocell and to investigate the effect of rubber-soil mixture layers between geocell layers on the behavior of reinforced system, the *h/D* ratio was subsequently maintained at 0.2.

6.3. The effect of the number of geocell layers on the behavior of the pavement foundation

The effect of the number of geocell layers on total deformation, permanent plastic deformation, and resilient displacement of loading plate, and on the pressure distributed through the pavement foundation bed (the results of Test Series 5) is the subject of this section. In this Test Series thirty loading and unloading cycles were applied. Fifteen first cycles and fifteen second cycles were applied to the loading plate with amplitudes of 400 and 800 kPa, respectively. As the preliminary tests had shown that 15 cycles of loading were sufficient to obtain a fully resilient response at the low level of cyclic pressure (400 kPa), the interest was to establish the likelihood of such a response being disturbed by a greater cyclic pressure (800 kPa) .

6.3.1. The effect of geocell layers on deformation of the pavement foundation

The variation of the loading plate deformation (including the accumulated residual (plastic) deformation and resilient (elastic rebound) displacement) with the number of load cycles for the unreinforced system and the multi-layered geocell reinforced system with one, two, three, and four layers of geocell (N_g=1, 2, 3, 4), when the layers of geocell were placed at the optimum values of *u/D* and *h/D* (*u/D*=*h/D*=0.2), is shown in Fig 8a. Also, the residual plastic deformation of the unreinforced and reinforced bases with the number of loading cycles is shown in Fig. 8b. This figure shows that for the unreinforced and reinforced bases, an initial, rapid total deformation (Fig. 8a) and rapid residual deformation (Fig. 8b) during the first load applications is followed by secondary deformation that develops at a slower rate. Both the total and plastic deformations caused by the first cycle of applied load form a large portion of the final deformation after all cycles. Overall, in most of the tests performed on the unreinforced and the geocell reinforced foundation, the initial, rapid deformation that took place due to the first cycle of loading gave rise to between 25% and 70% of the accumulated plastic deformation. This ratio is greater for the unreinforced foundation than for the reinforced foundation. The actual proportion appears to depend on the mass of reinforcement and on the magnitude of the applied cyclic load.

Fig. 8 shows that the total and residual deformations of the unreinforced pavement foundation material tend to increase with the number of load cycles. There is a non-stabilizing response; eventually leading to plastic failure, particularly at higher levels of cyclic loads (i.e., 800 kPa). The authors note that a large deformation in these tests is not the primary means of judging unsuitability of the arrangements under test but, rather, a non-stabilizing response. Large deformations could largely be dealt with in practice by compaction, whereas instability responses are destructive.

For the reinforced bases, regardless of the number of geocell layers, the rate of change of both total and the residual deformation of the loaded surface reduces as the number of load cycles increases, so that their response has become, approximately, stable after fifteen load cycles (of both 400 and 800 kPa applied load), particularly for the reinforced bases with three and four layers of geocell. The performance of geocell reinforcement in decreasing the deformations may be attributed to the superior confinement offered by the geocell layers in all directions. Thus the multi-cell geometry allows the soil in the cells to develop a passive resistance that increases the soil's bearing capacity and decreases the deformations within the pavement foundation. This behavior is a consequence of the shakedown process as the granular structure of the sand becomes arranged into a progressively more stable arrangement better able to behave resiliently without undergoing plastic deformation. It implies that the reinforced system as compared with unreinforced system (Fig. 8) is storing energy (and releasing it in resilient recovery) rather than the energy being used to cause further damage. This stabilizing response suggests that the early process of reorientation of particles inside the geocell layers, causing local fill stiffening, ceases relative rapidly and the system then reaches a "plastic shakedown" condition, in which subsequent deformation is fully recovered in each cycle. In such a case no yield condition is reached at conventional stress levels. The final deformation value can be referred to either as the "maximum deformation" or the "shakedown deformation (settlement)" (Werkmeister et al. (2001)). The behavioral patterns observed in these tests (Fig. 8) is in-line with those observed in the repeated load testing of unreinforced granular materials as observed by several authors (e.g. Werkmeister et al., 2001, 2005; Pérez et al., 2006) and as predicted from mechanical interaction considerations (García-Rojo and Herrmann, 2005).

From Fig. 8, it may be clearly observed that, as the number of geocell layers increases (i.e., the increase in the depth of the reinforced zone beneath the loading surface), both the peak and residual deformations of these pavement foundation installations decrease substantially. In order to have a clear comparison of the results for the unreinforced and multi-layered geocell reinforced bases, plots of the peak deformation and residual plastic deformation at load cycle number of 1, 5, 10, and 10 (n=1, 5, 10, 15), for the two applied load levels of 400 and 800 kPa, with the number of geocell layers (N_g) are shown in Fig. 9.

The results in Figs. 8 and 9 depict that, the maximum and residual deformations of the loading plate are considerably decreased relative to the unreinforced deformation as a consequence of the increase in the number of geocell layers, regardless of the level of applied repeated load and the load cycle number. For example, from Fig. 9b at 800 kPa amplitude of applied load and at load cycle number of 15, the residual deformation values are about 41.03, 33.02, 23.10, 17.43, and 15.39 mm for unreinforced bed, and reinforced bed with one, two, three and four layers of geocell, respectively. This example provides clear illustration how the rate of reduction in the residual plastic deformation (and also the total deformation, in Fig. 9a) reduces with increase in the number of geocell layers (N_g). Thakur et al. (2012) reported similar results of the total and residual deformations with number of loading cycles and with height of single geocell-reinforced bed.

No marked further decrease in the total and residual deformations would be expected, at both amplitudes of 400 and 800 kPa of cyclic load, if the number of geocell layers were to increase to 5 layers. Obviously, the greater number of geocell reinforcement layer may only be justified at the highest amplitude of cyclic load if at all.

The effect of the amplitude of the cyclic load on the deformations of the loading surface of unreinforced and geocell-reinforced foundations is clear from Fig. 8. As expected, the increase in the cyclic load magnitude causes a direct increase in deformation for both unreinforced and reinforced systems, irrespective of the number of geocell layers. Consider, for example, the residual plastic deformations for the reinforced bed with four layers of geocell (N_g=4). At the end of loading deformations are 5.53 and 15.39 mm for magnitudes of cyclic load that are 400 and 800 kPa, respectively. This example shows that the residual plastic deformation varies non-linearly with amplitude of load cycle (the deformation grew by a factor of about three whereas the amplitude of load cycle only doubled).

Also, from Fig. 9, it can be seen that the rate of enhancement in both maximum and residual plastic deformations decreases steadily with increase in the number of load cycles (the distance between the curves decreases with increase in the number of load cycles). Consequently, one can anticipate that the enhancement rates will become almost insignificant with further increase in the number of load cycles or in the number of geocell layers (N_g).

6.3.2. The effect of geocell layers on resilient displacement ratios

The resilient displacement (i.e. elastic rebound, defined as the difference between the deformation under loading and under the corresponding unloading condition), due to storing energy, plays a key role to decrease the accumulated residual plastic deformation of pavement foundation. To show this role, the variation of resilient displacement ratio during unloading cycles (defined as the ratio of resilient displacement at each cycle to the total deformation from the first cycle) for the unreinforced and geocell reinforced systems with one, two, three, and four layers of geocell, is shown in Fig. 10. This figure shows that, regardless of the mass of geocell reinforcement, the proportion of resilient displacement decreases rapidly during the first few loading cycles but stabilizes quickly to a constant value with increase in the load cycle number (probably indicative of a densifying effect). However, the reinforced pavement foundations show a much better performance (in decreasing the proportion of resilient displacement and promoting shakedown to a steady-state condition) with increase in the load cycle number as compared to the unreinforced base.

As anticipated, the reinforced base with four layers of geocell shows the highest proportion of resilient displacement while the unreinforced base shows the lowest proportion for all the pavement foundations tested. On the other hand, with increase in the number of geocell reinforcement layers, the proportion of resilient displacement increases, irrespective of the amplitude and number of load cycles. For example for the last cycle of loading and unloading (15th cycle of applied load level of 800 kPa), the resilient displacements are 4.63%, 11.47%, 15.75%, 20.70%, and 22.66% of the total deformation for unreinforced and reinforced beds with one, two, three, and four layers of geocell, respectively. A similar resilient response was reported for a recycled asphalt pavement base by Thakur et al. (2012) where the geocell significantly increased the proportion of deformation.

Overall, the tests results reveal that the geocell reinforcement improves the resilient behavior in addition to the reduction of the accumulated plastic and total deformation of the pavement foundation. It may be attributed to the increase in the rigidity of the system, restraining the soil against lateral movement with locking-up of the geocell framework.

6.3.3. The effect of geocell layers on stress in the pavement foundation

The variation of maximum measured stress with the number of load cycles, inside the foundation at the three levels of 190 mm (T.SPC) , 350 mm (M.SPC), and 510 mm (B.SPC) beneath the center of loading plate (see Fig. 4) for the unreinforced system and the multi-layered geocell reinforced system is illustrated in Fig. 11. For the unreinforced installation and the reinforced installation with one layer of geocell, the top, middle, and bottom soil pressure cells ("T.SPC", "M.SPC", and "B.SPC") are installed and the variation of soil pressure are measured during the cyclic load tests. In order to prevent damage to the soil pressure cells, for the reinforced bases with two layers of geocell, only the middle and bottom soil pressure cells ("M.SPC" and "B.SPC"), and for the reinforced bases with three layers of geocell, only the bottom soil pressure cells (B.SPC") are installed. For the reinforced bases with four layers of geocell, no pressure cells are installed.

The readings of the three soil pressure cells for unreinforced and reinforced bases show an immediate large increase in the vertical stress when the first cycle of loading is applied and then a further, smaller increase over the next 6-8 cycles of loading, thereafter stabilizing to a constant value. This pattern is observed irrespective of applied pressure or of cell depth.

The figure also demonstrates the performance of geocell layers, as anticipated, in reducing the pressure transferred through the pavement foundation. For instance, as can be seen in Fig. 11c, with increase in the number of geocell layers from one layer to three, the vertical stress transferred to a depth of 510 mm beneath the center of loading surface, as measured by the bottom soil pressure cell ("B.SPC"), almost halves. For example, under the applied cyclic pressure of 800 kPa, at the end of the load cycles (cycle number 30), the stress measured at 510 mm depth ("B.SPC") is about 284.5, 223.5, 159.7, 125.2 kPa for unreinforced and the reinforced pavement foundations with one, two and three layers of geocell, respectively. This comparison illustrates the excellent performance of the geocell reinforcement, so that the pressure at a depth of 510 mm decreases to about 35.6%, 27.9%, 20%, and 15.7% of the applied surface pressure (=800 kPa) for the same sequence of constructions. Thus as reinforcing geocell layers are added, the effective load spreading continues to improve, consequently delivering a better performance, as compared with unreinforced base. On the whole, the data presented in Figs. 11 and Fig. 9 (variation of residual plastic deformation with the number of geocell layers) show that multiple geocell layers, particularly the use of three and four layers of geocell, are able to limit the soil surface deformation and the soil pressure through the depth of the reinforced pavement foundation. Consequently an increase in road life may be anticipated under the same heavy traffic loading.

Considering both the deformation and stress effect, it appears that, cell-pocket structure of the geocell layer prevents the encased soil from easily moving away from the point of load application. Very probably, this is achieved by hoop confinement provided by the pocket walls. Thereby the infill cannot easily spread laterally; hence the shear strength of the composite system is increased.

This mechanism would allow the geocell layer to act like a soft plate with high flexural stiffness, spreading the applied load over an extended area, and decreasing the stress at depth in the pavement foundation (Moghaddas Tafreshi and Dawson, 2012; Thakur et al., 2012). This stated another way; the geocell seems able to effectively attenuate the vertical applied stress in the soil because it provides a good connection between the loaded area and anchorages on both sides of the loaded area (Tavakoli et al., 2012).

6.4. The combined effect of geocell layers and rubber-soil mixture layers

To investigate the beneficial effect of mixing reinforcing rubber with soil so as to improve the response of the pavement foundations to cyclic load, this section concentrates on comparing the effect of multiple layers of geocell reinforcement system with inter-layer rubber reinforced soil The tests combined of the same number of layers of each reinforcement type (N_g=N_{rs}=1; N_g=N_{rs}=2; N_g=N_{rs}=3 and N_g=N_{rs}=4). To evaluate the response, each combined installation is compared to comparable geocell-only installation, i.e. N_g=1 is compared to N_g=N_{rs}=1, N_g=2 to N_g=N_{rs}=2, N_g=3 to N_g=N_{rs}=3, and N_g=4 to N_g=N_{rs}=4.

6.4.1. The effect of rubber-soil mixture with geocell layers on deformation of pavement foundations

Fig. 12 compares the variation of the loading plate deformation with the number of load cycles for the unreinforced system, the multi-layered geocell reinforced system and combined geocell and rubber-reinforced system. To more clearly demonstrate the performance of the rubber-reinforced soil layers, the same data, but only the residual plastic deformation, is shown in Fig. 13. From these figures, it can clearly be observed that replacing the unreinforced soil beneath the geocell layers with a rubber reinforced soil layer considerably decreases both the total and residual plastic deformations of the loading plate, compared with the response of the unreinforced bed and geocell-reinforced bed, irrespective of the number of reinforcement layers, the level of applied repeated load or the load cycle number.

For a more quantitative comparison, and to show more clearly the effect of the rubber soil mixture on the behavior of foundation bed, the values of maximum and residual plastic deformations, as well as the proportion of deformations that are recoverable (i.e., resilient), are tabulated in Table 4. These values are shown for the last cycle of loading (15th load cycle) of the two levels of applied cyclic loads (= 400 and 800 kPa).

The data presented as Table 4 shows clearly that, as anticipated, both the peak and residual plastic deformations decrease and the proportion of the deformation that is resilient increases with the number of geocell layers. The further benefit to the deformation behavior of combining geocell with granulated rubber-soil layers is also evident. Comparison of the deformation performance of the combined rubber-soil and geocell layer installations with those reinforced by geocell layers alone, reveals that the addition of the rubber treatment cause both the maximum and the residual (plastic) deformations to decrease substantially. For example, consider the second row within the 800 kPa loading section of Table 4 and the N_g=3 / N_g=N_{rs}=3 cases in this row. In this comparison the residual, plastic, deformation of the pavement foundation reinforced by three geocell layers drops by about 57% compared to that of the unreinforced case and by 68% when reinforced with three layers of geocell and three layers of rubber-soil mixture. For the same installations, the last row in Table 4 shows that all the reinforced installations exhibit greater proportion of deformations (that is resilient) than does the unreinforced pavement foundation and that the combined geocell and rubber reinforcement layers increase the proportion of deformations from the values obtained for the geocell layers-only installation. Thus all the reinforced installations appear to reduce plastic deformations, in part, by storing energy in resilient deformation, but this effect is increased by the addition multiple rubber-treated soil layers. Given the reduction in plastic deformation at the same time as the resilient deformation increases, it follows that the pavement foundations are becoming much more resilient installations – the proportion of deformations increases by about 2.5-5 times over that of the unreinforced installation, irrespective of the reinforcement type or applied load. As energy is absorbed through the deformation of the rubber particles themselves (Feng and Sutter, 2000, Tavakoli Mehrjardi et al., 2012), it is, perhaps, surprising that the addition of the rubber in the study described here does not lead to much greater deformations as a result of the reinforcement effect of the rubber in the mixture.

6.4.2. The effect of rubber-soil mixture with geocell layers on pressure distribution

Fig. 14 illustrates the variation of stress inside the pavement foundation bed at two depths, 190 and 350 mm, beneath the center of loading plate ("T.SPC" and "M.SPC" in Fig. 4), with the number of load cycles. Results are presented for the unreinforced, the geocell-reinforced and the combination reinforced pavement foundations. Due to equipment availability and the need to protect them from stress concentrations, it was not possible to monitor the stresses at all depths in all installations.

Fig. 14 depicts a further aspect of the improvement caused by the treatments – the reduction in stress with depth. For example, as can be seen in Fig. 14b, for the applied cyclic pressure of 400 kPa at the soil surface, by the end of the 15th load cycle the pressure at a depth of 350 mm measured by the middle soil pressure cell ("M.SPC") is about 181.1, 120.1, and 75.30 kPa for unreinforced, reinforced bed with two layers of geocell (N_g=2), and the combined rubber and geocell-reinforced bed (two layers of each: N_g=N_{rs}=2), respectively. The values above are about 0.45, 0.3, and 0.19 times the applied surface pressure of 400 kPa, with the installation containing the combination two geocell and two rubber-soil mixture layers (N_g=N_{rs}=2) delivering a 37.3% reduction in stress compared with the performance offered by the installation with two geocell layers only (N_g=2).

Thus the addition of the rubber-soil mixture effect allows more load-spreading, consequently delivering an improved performance. The beneficial effect of the rubber-soil mixture beneath the geocell layers may be attributed to two reasons:

(1) the granulated rubber has a reinforcement effect, although the reasons for this are not clear. It may be that the particle-scale heterogeneity allows tensile loads to be carried between granular particles via adjacent, extensible, rubber particles. It may be for some other reason;

(2) the rubber-soil mixture layer is able to absorb more energy than the soil alone. Consequently, plastic deformations are reduced and load spreading increased, the latter effect leading to reduction of stress with depth.

In addition, to the benefits identified above, the inclusion of rubber would also, in principle, cause considerable increase in environmental and economic benefits by reusing otherwise waste rubber. Despite the benefits identified, it is expected that the contribution of the rubber to the treated soil's performance will be highly dependent on the size of the rubber fragments, the type of rubber and the proportion added to the soil.

7. Summary and conclusion

A series of cyclic plate load tests was conducted to assess the concept of geocell-reinforced layers and rubber-soil mixture layers as potential pavement foundation improvement techniques. Based on the results of the test program described in this paper, the following conclusions can be made:

(1) The optimum embedded depth of the first layer of geocell beneath the loading plate and the optimum vertical spacing of geocell layers, under repeated loads, based on plate settlement, are both approximately 0.2 times loading plate diameter ($u/D \approx h/D \approx 0.2$).

(2) With increase in the number of load cycles, the maximum and plastic deformations tend to increase. For two levels of amplitude of cyclic load (400 kPa and 800 kPa), a large proportion of the total deformation (25-70%) occurred during the first cycle of load. The actual proportion appears to depend on the mass of reinforcement and on the magnitude of the applied cyclic load.

(3) The rate at which further deformation then accumulates is much slower than under the first few cycles of loading. If or when deformation accumulation ceases altogether, then a resilient response condition, known as plastic shakedown, may be achieved. Its occurrence appears to depend on both the mass of reinforcement and the magnitude of the cyclic load applied to the loading plate.

- At the low level of cyclic load (400 kPa), under fifteen load cycles applied to the loading plate, plastic shakedown occurs in all installations, irrespective of the reinforcement mass beneath the loading surface.
- At the high level of cyclic load (800 kPa), for the test performed on the unreinforced pavement foundation, the surface deformation is relatively large and non-stabilizing at the end of cyclic

loading. For the tests performed with a high reinforcement mass (N_g=3, 4 and N_g=N_{rs}=3, 4), plastic shakedown occurs. When using the low (N_g=1 and N_g=N_{rs}=1) and moderate (N_g=2 and N_g=N_{rs}=2) reinforcement mass, the rate at which deformation accumulates under cyclic loading is significantly reduced. Shakedown was not experienced during the testing (15 cycles) but is anticipated after further cycling.

(4) As the number of geocell and rubber-soil mixture layers increases, the loading surface deformation of the pavement foundation decreases due, in part, to better load spreading of the composite system. Combined geocell layers and rubber soil mixture layers reinforce the pavement foundation more effectively – reducing the surface deformation – than the same number of geocell layers acting alone. Under the last cycle of loading at 800 kPa with three layers of geocell (N_g=3), the residual, plastic, deformation is only about 42% of the value for the unreinforced case and this ratio drops to only 32% when the same number of rubber-soil layers (N_g=N_{rs}=3) is added.

(5) After several load cycles, for the reinforced beds, the proportion of deformation bed that is resilient tends to a constant value due to densification, irrespective of mass, type or number of reinforcements. Ultimately, only resilient deformation is observed during a cycle of loading. Shakedown has then been achieved.

(6) Resilient deformation forms a greater proportion of the total deformation as the number of geocell and rubber-soil mixture layers increases. The combined geocell and rubber-soil layers are most effective at increasing the proportion of deformation that is resilient, presumably due to the elastic property of the rubber particles that were added.

(7) The vertical stress that is spread through the pavement foundation, takes several cycles before reaching a level at which it becomes approximately constant.

(8) The inclusion of the geocell and rubber-soil mixture layers beneath the loading plate acts to prevent the punching shear observed in the surface of unreinforced installation and leads to significant reduction in the vertical stress spread through the pavement foundation by distributing the load over a wider area. At a depth about 2/3^{rds} of the loaded plate diameter, the vertical stress was about 97% of the applied 800 kPa stress when

the foundation was unreinforced and only about 73% of this value when reinforced with one layer of geocell and one layer of rubber-soil mixture (N_g=N_{rs}=1).

(9) Under cyclic loading, use of the combined geocell and rubber soil mixture layers is more effective than geocell layers alone in reducing the stress distributed down into the pavement foundation. At a depth, a little greater than the loading plate diameter (i.e., depth of 350 mm), the vertical stress transferred from a cyclic surface load of 800 kPa is reduced by 41% when two geocell layers and two rubber-soil mixture layers (N_g=N_{rs}=2) are combined compared with the stress at the same point when two geocell layers (N_g=2) are used alone.

The results provide considerable encouragement for the use of multiple layers of geocell reinforcement, especially in combination with inter-layers of rubber-soil mixture, for addressing localized soft pavement foundation conditions. The tests results are obtained for only one type of soil, one type of geocell with one pocket size, one type and size of rubber, and one load diameter. Generalization may be needed, therefore, before these findings may be directly applied. Using rubber reinforcement derived from scrap tires as a reinforcing agent has the potential to deliver considerable environmental and economic benefit, although economic assessments of the production and placement of soil-rubber mixtures, together with geocells, at commercial scale would need to be performed to assure users of the applicability of the findings in every situation.

Acknowledgements

The geocell used in this study was provided by DuPont de Nemours Company in the UK (the holder of the trademark on the GroundGrid™ and Typar® products). Also, Dr. T. Amirsoleymani, the managing director of Mandro Consulting Engineer, in Iran and their technicians provided the loading system, pit and some of the instrumentations and provided great assistance during the tests. The authors appreciate all the above support.

References

Abu-Farsakh, M., Chen, Q., Yoon, S., 2008. Use of Reinforced Soil Foundation (RSF) to Support Shallow Foundation, Final Report. Louisiana Transportation Research Center (LTRC), Louisiana Department of Transportation and Development (LADOTD), Baton Rouge, LA, Report No. FHWA/LA.07/424, 195 pp.

American Society for Testing and Materials. 2009. Standard Test Method for Repetitive Static Plate Load Tests of Soils and Flexible Pavement Components, for Use in Evaluation and Design of Airport and Highway Pavements. ASTM, D 1195-09.

American Society for Testing and Materials, 2009. Standard Specification for Graded Aggregate Material for Bases or Subbases for Highways or Airports. ASTM, D2940-09.

American Society for Testing and Materials, 2011. Standard Practice for Classification of Soils for Engineering Purposes (Unified Soil Classification System). ASTM International, West Conshohocken, PA, D 2487-11.

American Society for Testing and Materials, 2012. Standard Test Methods for Laboratory Compaction Characteristics of Soil Using Modified Effort. ASTM, D 1557-12.

American Association of State Highway and Transportation Officials (AASHTO) T 221-90. Repetitive static plate load tests of soils and flexible pavement components for use in evaluation and design of airport and highway pavements.

Attom, M.F., 2006. The use of shredded waste tires to improve the geotechnical engineering properties of sands. Environmental and Geology, 49 (4), 497–503.

Bathurst, R.J., Nernheim, A., Walters, D.L., Allen, T.M., Burgess, P., Saunders, D.D., 2009. Influence of reinforcement stiffness and compaction on the performance of four geosynthetic – reinforced soil walls. Geosynthetics International, 16 (1): 43–49.

Bosscher PJ, Edil TB, Kuraoka S. Design of highway embankments using tire 666 chips. J Geotech Geoenviron Eng ASCE 1997;123(4):295–304.

Boushehrian A.H., Hataf, N., Ghahramani, A., 2011. Modeling of the cyclic behavior of shallow foundations resting on geomesh and grid-anchor reinforced sand. Geotextiles and Geomembranes 29 (3), 242-248.

Brito, L.A.T., Dawson, A.R., Kolisoja, P.J., 2009. Analytical evaluation of unbound granular layers in regard to permanent deformation. In: Proceedings of the 8^{th} International on the Bearing Capacity of Roads, Railways, and Airfields (BCR2A'09), Champaign IL, USA, pp. 187-196.

Cetin, B., Aydilek, A.H., Li, L., 2012. Experimental and numerical analysis of metal leaching from fly ash-amended highway bases. Waste Management. 32(5), 965-978

Chen, R.H., Huang, Y.W., Huang, F.C., 2013. Confinement effect of geocells on sand samples under triaxial compression Geotextiles and Geomembranes 37 (2), 35-44.

Chiu, C.T., 2008. Use of ground tire rubber in asphalt pavements: field trial and Evaluation in Taiwan. *Journal of Resources, Conservation and Recycling*. 52 (3), 522–532.

Dash S.K, Sireesh S, Sitharam T.G., 2003. Model studies on circular footing supported on geocell reinforced sand underlain by soft clay. Geotextiles and Geomembranes 21 (4), 197–219.

Dash, S.K., Rajagopal, K., Krishnaswamy, N.R., 2007. Behaviour of geocell reinforced sand beds under strip loading. Canadian Geotechnical Journal. 44 (7), 905–916.

Edincliler, A., Baykal, G., Dengili K., 2004. Determination of static and dynamic behavior of recycled materials for highways. Resources Construction and Recycling. 42 (3), 223-237.

Edincliler, A.. Cagatay, A., 2013. Weak subgrade improvement with rubber fibre inclusions. Geosynthetics International, 20 (1), 39-46.

Feng, Z. Y., & Sutter, K. G., 2000. Dynamic properties of granulated rubber sand mixtures. Geotechnical Testing Journal, 23, No.3, 338–344.

García-Rojo, R., Herrmann, H.J., 2005. Shakedown of unbound granular material. Granular Matter 7 (2), 109-118.

Hufenus, R., Rueegger, R., Banjac, R., Mayor, P., Springman, S.M., Bronnimann, R., 2006. Full-scale field tests on geosynthetic reinforced unpaved on soft subgrade. Geotextiles and Geomembranes 24 (1) 21–37.

Kim, I.T. and Tutumluer, E., 2005. Unbound Aggregate Rutting Models for Stress Rotations and Effects of Moving Wheel Loads. Transportation Research Record, Journal of the Transportation Research Board 1913, 41–49.

Koerner, R.M., 2012. Designing with geosynthetics. 6th Edition Vol. 1. Xlibris Corporation. USA.

Lambert, S., Nicot, F., Gotteland, P., 2011. Uniaxial compressive behavior of scrapped tire and sand-filled wire netted geocell with a geotextile envelope. Geotextiles and Geomembranes, 29, (5), 483-490.

Leshchinsky, B., & Ling, H. I. (2013). Numerical modeling of behavior of railway ballasted structure with geocell confinement. Geotextiles and Geomembranes, 36 (1), 33–43.

Lovisa, J., Shukla, S.K., Sivakugan, N., 2010. Shear strength of randomly distributed moist fiber-reinforced sand. Geosynthetics International 17 (2), 100–106.

Madhavi Latha, G., Somwanshi, A., 2009. Bearing capacity of square footings on geosynthetic reinforced sand. Geotextiles and Geomembranes 27 (4), 281–294.

Munnoli, P.M., Sheikh, S., Mir, T., Kesavan, V. & Jha, R., 2013, Utilization of rubber tyre waste in subgrade soil, Global Humanitarian Technology Conference: South Asia Satellite (GHTC-SAS), 330-333.

Moghaddas Tafreshi, S.N., Dawson, A.R., 2012. A comparison of static and cyclic loading responses of foundations on geocell-reinforced sand. Geotextiles and Geomembranes, 32 (5), 55-68.

Moghaddas Tafreshi, S.N., Tavakoli Mehrjardi, GH., Dawson, A.R., 2012. Buried pipes in rubber-soil backfilled trenches under cyclic loading. Journal of Geotechnical and Geoenvironmental Engineering, ASCE, 138 (11) 1346-1356.

Moghaddas Tafreshi, S.N., Khalaj, O., Dawson, A.R., 2013. Pilot-scale load tests of a combined multi-layered geocell and rubber-reinforced foundation. Geosynthetics International, 20 (3), 143–161.

Palmeira, E.M., Andrade, H.K.P.A., 2010. Protection of buried pipes against accidental damage using geosynthetics. Geosynthetics International, 17 (4), 228–241.

Pokharel, S. K., Han, J., Leshchinsky, D., Parsons, R. L., Halahmi, I., 2010. Investigation of factors influencing behavior of single geocell-reinforced bases under static loading. Geotextiles and Geomembranes 28 (6), 570-578.

Prasad, D.S.V., Prasada Raju, G. V. R., 2009. Performance of waste tyre rubber on model flexible pavement. ARPN, Journal of Engineering and Applied Sciences 4 (6), 89-92.

Pérez, I., Medina, L., Romana, M.G., 2006. Permanent deformation models for a granular material used in road pavements. Construction and Building Materials 20 (9), 790-800.

Rubber Manufacturers Association, RMA. <http://www.rma.org>; 2007 [accessed 05.07.11].

Recycling Research Institute, RRI. <http://www.scraptirenews.com>; 2009 [accessed 05.07.11].

Sitharam, T.G., Sireesh, S., 2005. Behavior of embedded footings supported on geogrid cell reinforced foundation beds. Geotechnical Testing Journal 28 (5), 452-463.

Sitharam, T.G., Sireesh, S.,Dash, S.K., 2007. Performance of surface footing on geocell-reinforced soft clay beds. Geotechnical and Geological Engineering. 25 (5), 509–524.

Sireesh, S., Sitharam, T.G., Dash, S.K., 2009. Bearing capacity of circular footing on geocell–sand mattress overlying clay bed with void. Geotextiles and Geomembranes 27 (2), 89–98.

Tanchaisawat, T., Bergado, D.T., Voottipruex, P., Shehzad, K., 2010. Interaction between geogrid reinforcement and tire chip–sand lightweight backfill. Geotextiles and Geomembranes. 28 (1), 119-127.

Tanyu, B. F., Aydilek, A. H., Lau, A. W., Edil, T. B., Benson, C. H. (2013). Laboratory Evaluation of Geocell-Reinforced Gravel Subbase Over Poor Subgrades. Geosynthetics International, 20(2), P.47 –61

Tavakoli Mehrjardi, Gh., Moghaddas Tafreshi, S.N., Dawson, A.R., 2012. Combined use of geocell reinforcement and rubber–soil mixtures to improve performance of buried pipes. Geotextiles and Geomembranes. 34 (October), 116-130.

Thakur, J.K., Han, J., Pokharel, S.K., Parsons, R.L., 2012. Performance of geocell-reinforced recycled asphalt pavement (RAP) bases over weak subgrade under cyclic plate loading. Geotextiles and Geomembranes 35 (December), 14-24.

Yang, X., Han, J., Pokharel, S.K., Manandhar, C., Parsons, R.L., Leshchinsky, D., Halahmi, I., 2012. Accelerated pavement testing of unpaved roads with geocell-reinforced sand bases. Geotextiles and Geomembranes 32, (June), 95-103

Yoon, Y. W., Heo, S. B., Kim, S. K., 2008. Geotechnical performance of waste tires for soil reinforcement from chamber tests. Geotextiles and Geomembranes 26 (1), 100-107.

Werkmeister, S., Dawson, A.R., Wellner, F., 2001. Permanent deformation behaviour of granular materials and the shakedown theory. Journal of Transportation Research Board 1757, 75-81.

Werkmeister, S., Dawson, A.R., Wellner, F., 2005. Permanent deformation behaviour of granular materials. International Journal of Road Materials and Pavement Design 6, 31-51.

Waste and Resources Action Programme, WRAP. Tyres re-use and recycling, <http://www.wrap.org.uk>; 2007 [accessed 05.07.11].

Zhang, L., Zhao, M., Shi, C., Zhao, H., 2010. Bearing capacity of geocell reinforcement in embankment engineering. Geotextiles and Geomembranes 28, (5), 475-482.

Nomenclature

b	Width of the both geocell and rubber-soil mixture layers
C_u	Coefficient of uniformity
C_c	Coefficient of curvature
D	Loading plate diameter
D_{10}	Effective grain size (mm)
D_{30}	Diameter through which 30% of the total soil mass is passing (mm)
D_{60}	Diameter through which 60% of the total soil mass is passing (mm)
G_s	Specific gravity of soil
d	Geocell pocket size
φ	Angle of shearing resistance of soil being reinforced
u	Embedded depth of the geocell
H_g	Height of geocell layers
h	Vertical spacing of the geocell layers
h_{rs}	Height of the rubber-soil mixture layers
N_g	Number of geocell reinforcement layers
N_{rs}	Number of soil-rubber mixture reinforcement layers
SPC	Soil pressure cell
T.SPC	Top Soil Pressure Cell
M.SPC	Middle Soil Pressure Cell

B.SPC Bottom Soil Pressure Cell

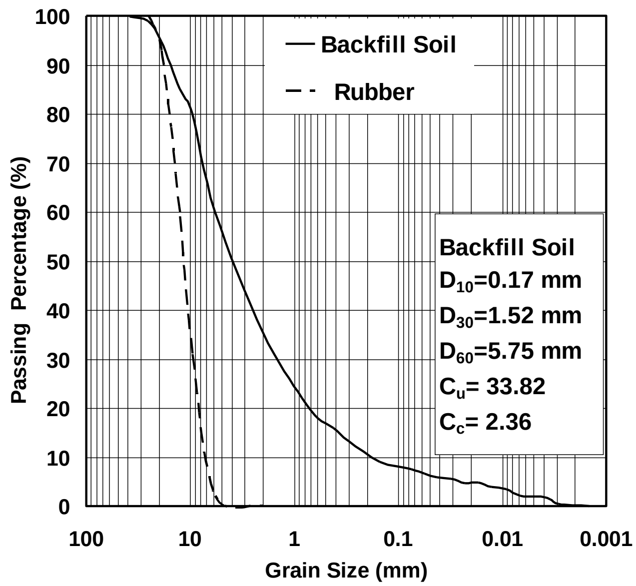

Fig. 1. Particle size distribution curves for backfill soil and granulated rubber (determined according to ASTM D422-07)

Fig. 2. A view of geocell (TDP Limited) spread over soil/soil-rubber in the test pit.

Fig. 3. A view of granulated tire rubber used.

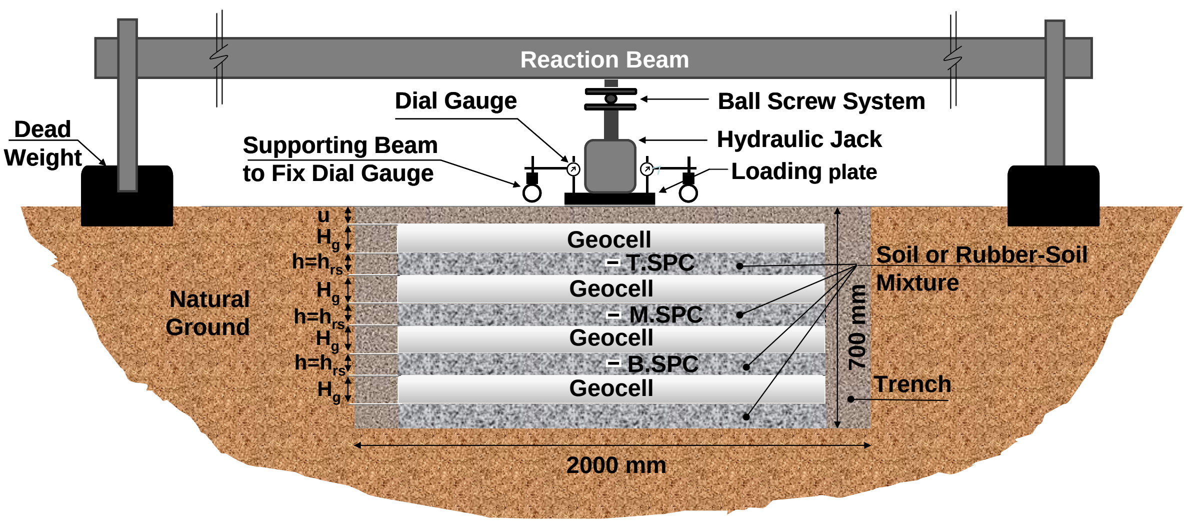

Fig. 4. Schematic cross-section of the test set-up (not to scale), "T.SPC", "M.SPC", and "B.SPC" indicate the location of soil pressure cells.

Fig. 5. Photograph of test installation prior to loading include reaction beam, load plate, hydraulic jack and three dial gauges.

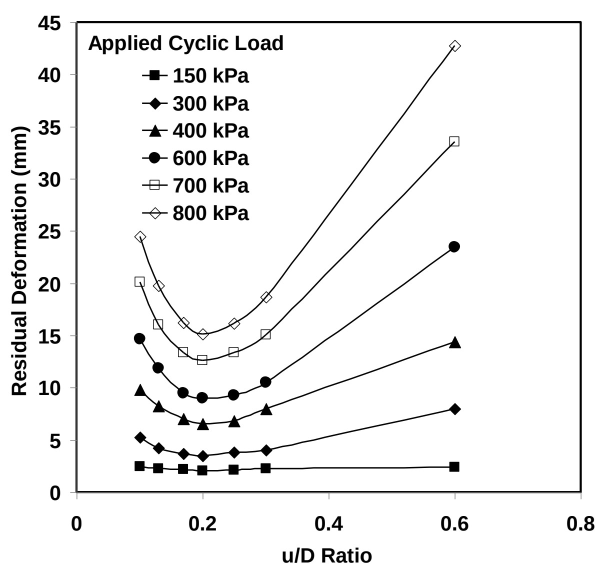

Fig. 6. Variation of residual plastic deformation with *u/D* ratio at different amplitudes of cyclic load.

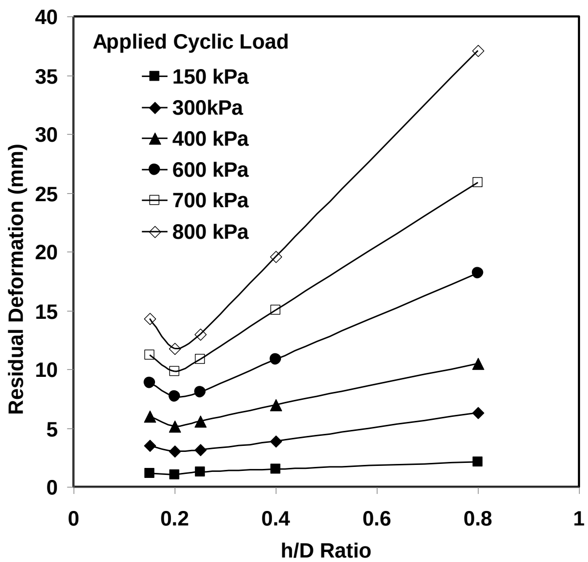

Fig. 7. Variation of residual plastic deformation with *h/D* ratio at different amplitudes of cyclic load.

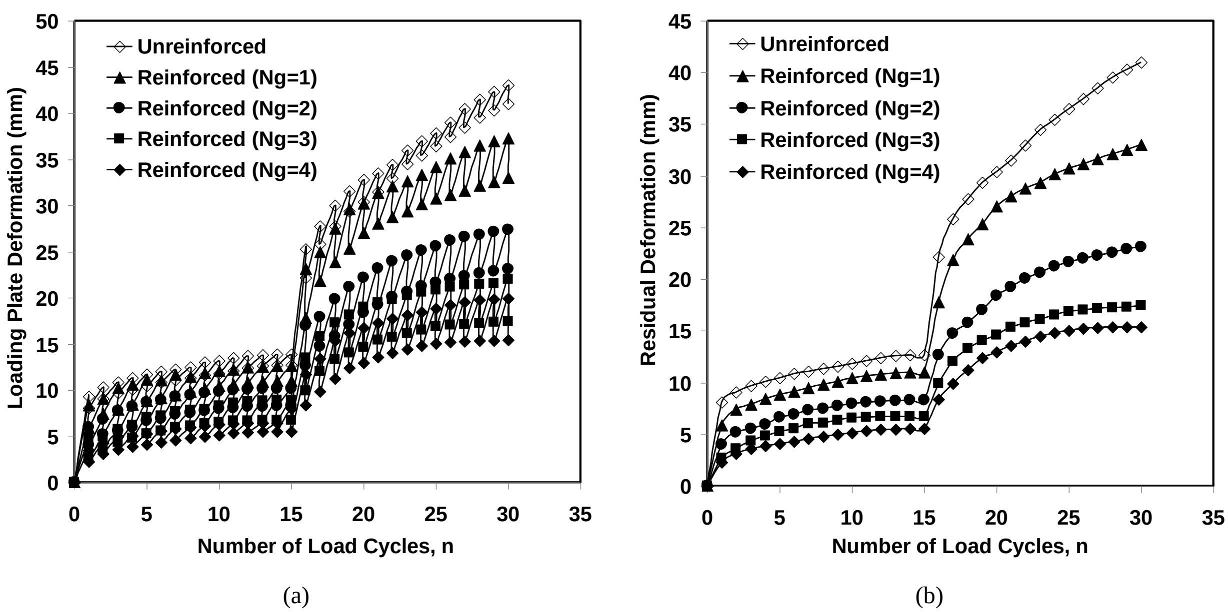

Fig. 8. Variation of (a) loading plate deformation, and (b) residual deformation with number of applied load cycles for the unreinforced and geocell reinforced systems with one, two, three, and four layers of geocell. The fifteen first cycles and the fifteen second cycles were applied with amplitudes of 400 and 800 kPa, respectively.

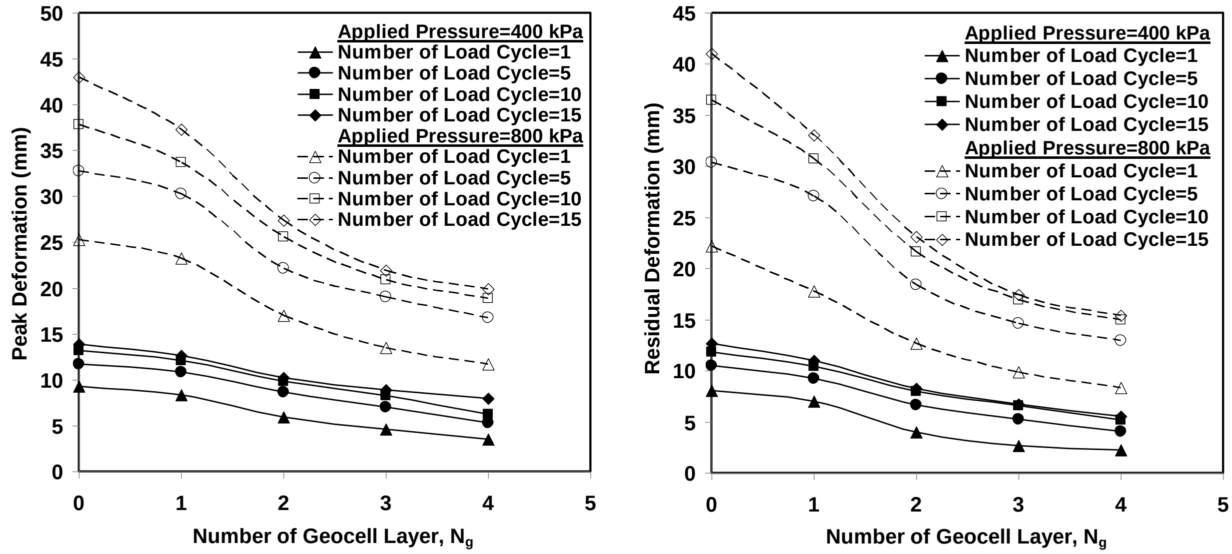

(a) (b)

Fig. 9. Variation of (a) peak, and (b) residual deformation with number of geocell layers for two levels of applied repeated load (400 and 800 kPa) at load cycle of 1, 5, 10, and 15.

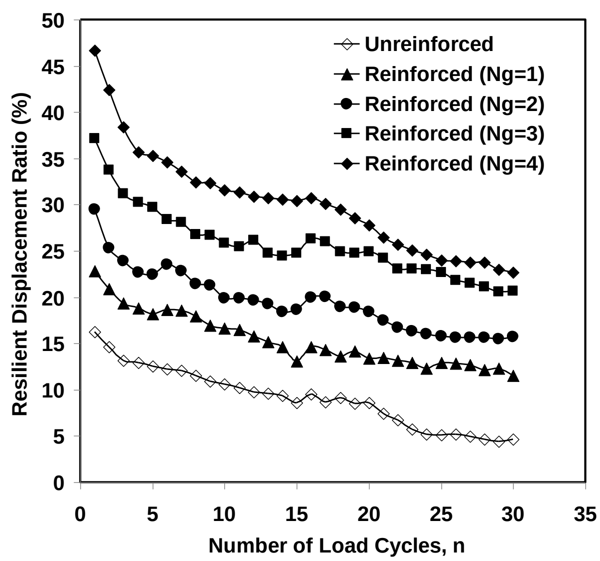

Fig. 10. Variation of resilient displacement ratio with number of applied load cycles for the unreinforced and geocell reinforced systems with one, two, three, and four layers of geocell. The fifteen first cycles and the fifteen second cycles were applied with amplitudes of 400 and 800 kPa, respectively.

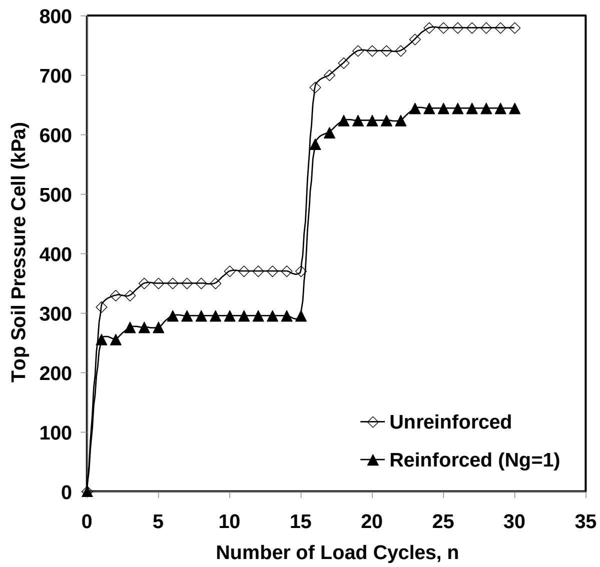

(a)

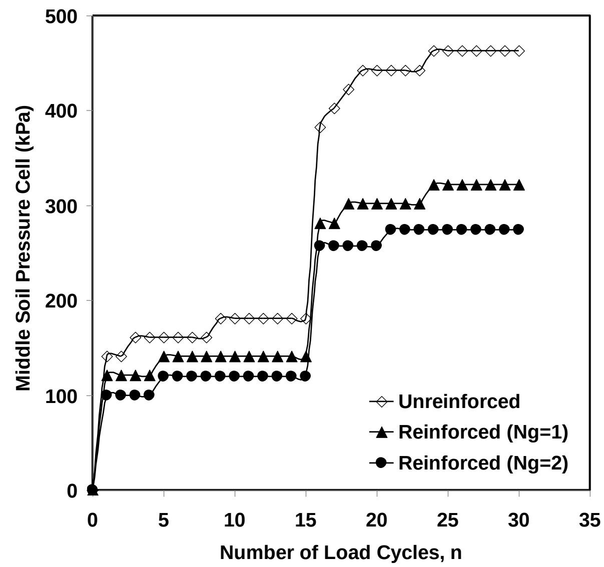

(b)

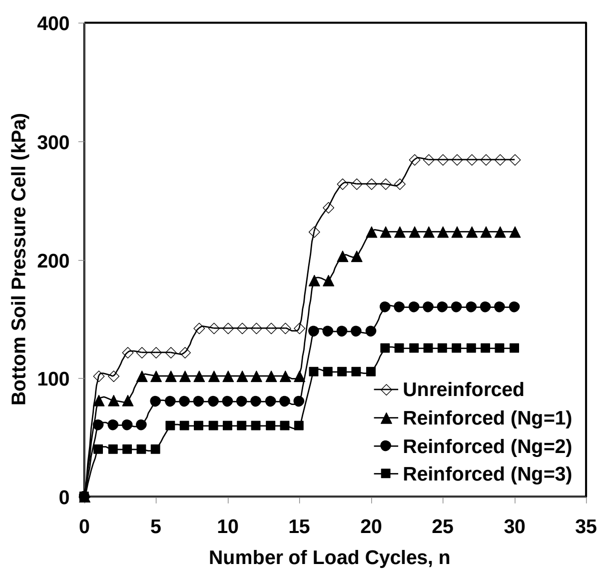

(c)

Fig. 11. Variation of transferred pressure with number of applied load cycles at different depths in the geocell-reinforced and unreinforced pavement foundations (a) at a depth of 190 mm (T.SPC), (b) at a depth of 350 mm (M.SPC), and (c) at a depth of 510 mm (B.SPC). The fifteen first cycles and the fifteen second cycles were applied with amplitudes of 400 and 800 kPa, respectively.

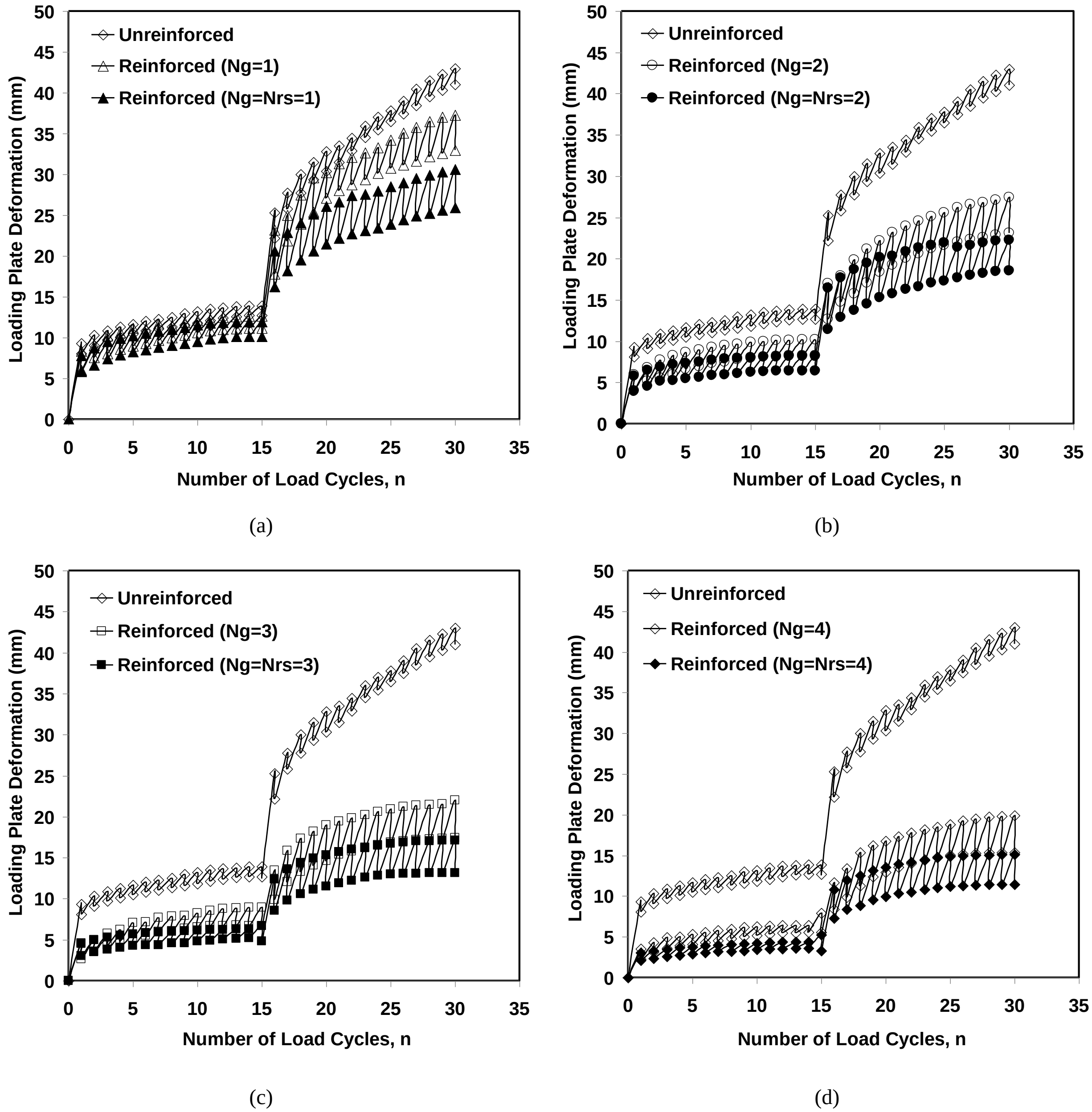

Fig. 12. Variation of loading plate deformation with number of applied load cycles for the unreinforced, geocell reinforced, and combined geocell and rubber-reinforced systems (a) N_g=1 and N_g=N_{rs}=1, (b) N_g=2 and N_g=N_{rs}=2, (c) N_g=3 and N_g=N_{rs}=3, and (d) N_g=4 and N_g=N_{rs}=4. The fifteen first cycles and the fifteen second cycles were applied with amplitudes of 400 and 800 kPa, respectively.

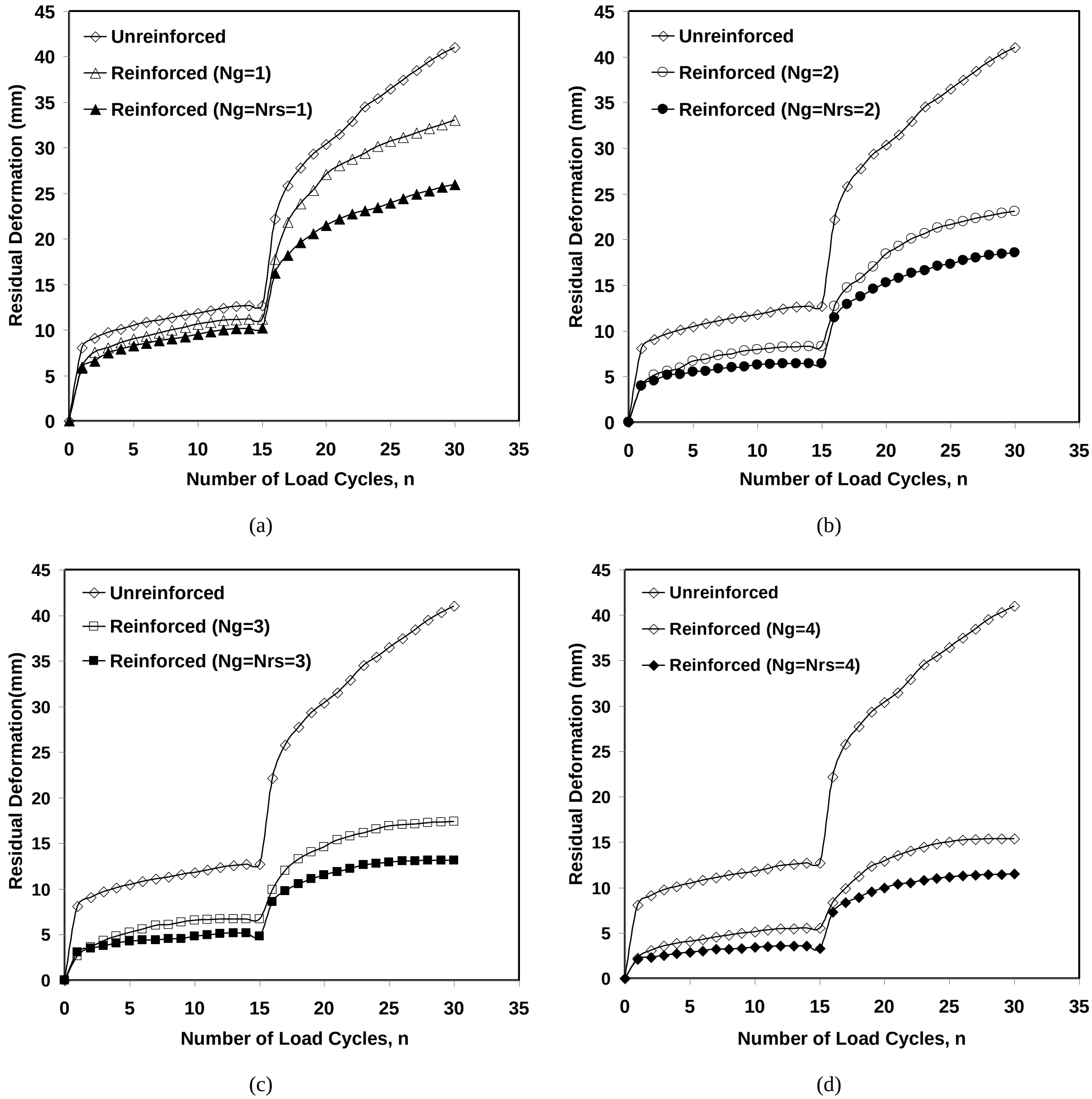

Fig. 13. Variation of residual plastic deformation with number of applied load cycles for the unreinforced, geocell reinforced, and combined geocell and rubber-reinforced systems (a) N_g=1 and N_g=N_{rs}=1, (b) N_g=2 and N_g=N_{rs}=2, (c) N_g=3 and N_g=N_{rs}=3, and (d) N_g=4 and N_g=N_{rs}=4. The fifteen first cycles and the fifteen second cycles were applied with amplitudes of 400 and 800 kPa, respectively.

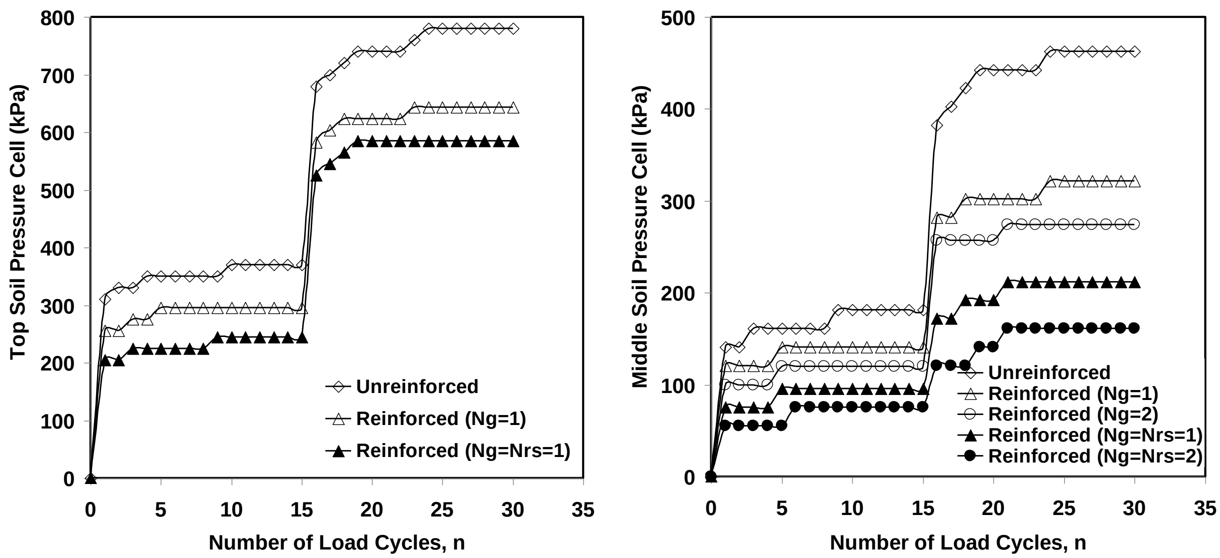

(a) (b)

Fig. 14. Variation of stress in the pavement foundation with number of applied load cycles at different depths for unreinforced, geocell-only-reinforced and combined geocell and rubber-reinforced soil (a) at depth of 190 mm (T.SPC), (b) at depth of 350 mm (M.SPC). The fifteen first cycles and the second fifteen cycles were applied with amplitude of 400 and 800 kPa, respectively.

Table 1

The engineering properties of the geotextile used in the tests.

Description	**Value**
Type of geotextile	Non-woven
Material	Polypropylene
Mass per unit area (gr/m^2)	190
Thickness under 2 kN/m^2 (mm)	0.57
Thickness under 200 kN/m^2 (mm)	0.47
Tensile strength (kN/m)	13.1
Strength at 5% (kN/m)	5.7
Effective opening size (mm)	0.08
Height of cells, H_g (mm)	100
Geocell pocket size (Width and length of cells), *d* (mm)	110

Table 2

Densities of different materials after compaction (ASTM D 1557-12).

Type of material	**Rubber content (%)**	**Dry density (kN/m^3)**
Unreinforced soil layer	No rubber	≈18.56*
Geocell reinforced layer	No rubber	Between 18 and 18.5
Rubber-soil mixture layer	8	≈13.6

* approximately 90% of maximum dry density – see Section 3.1

Table 3

Scheme of the cyclic plate load tests for unreinforced pavement, multi-layered geocell pavement and combined multi-layered geocell and rubber-reinforced pavement.

Test Series	**Type of test**	***N_g***	***N_{rs}***	***u/D***	***h/D .OR. h_{rs}/D***	**No. of Tests**	**Purpose of the tests**
1	Unreinforced	--------	--------	-------		1+2*	To quantify the improvements due to reinforcements
**2	Geocell reinforced	1	-------	0.1, 0.13, 0.17, 0.2, 0.25, 0.3, 0.6	-------	7+3*	To arrive at the optimum values of u/D and h/D
**3		2	-------	0.2	0.15, 0.2, 0.25, 0.4, 0.8	5+2*	
4		1, 2, 3, 4	-------	0.2	0.2	4+2*	To study the effect of the number of geocell layers
5	Geocell Reinforced + Rubber-soil mixture	1	1	0.2	0.2	4+4*	To investigate the effect of combined use of geocell reinforcement and rubber-soil mixtures.
		2	2				
		3	3				
		4	4				

**The tests which were performed two or three times to verify the repeatability of the test data*

***in order to save time, only one load cycle of 150, 300, 400, 600, 700, and 800 kPa pressure were applied.*

Table 4. The maximum deformation, residual deformation, and proportion of deformation (that is resilient) of unreinforced bed, reinforced bed with geocell layers, and reinforced bed with combination of geocell and rubber-soil mixture layers at the last cycle of loading (15th load cycle) of two levels of applied loads (= 400 and 800 kPa).

Applied cyclic load	**Parameters**	**Unreinforced bed**	**Reinforced bed with geocell**				**Reinforced bed with geocell and rubber**			
			N_g=1	N_g=2	N_g=3	N_g=4	N_g=N_{rs}=1	N_g=N_{rs}=2	N_g=N_{rs}=3	N_g=N_{rs}=4
400 kPa	Maximum deformation (mm)	13.90	12.63	10.18	8.92	7.95	11.98	8.21	6.68	5.25
	Residual plastic deformation (mm)	12.70	10.98	8.28	6.71	5.53	10.19	6.45	4.84	3.33
	Proportion of deformation that is resilient (%)	8.63	13.07	18.66	24.77	30.44	14.94	21.44	27.55	36.57
800 kPa	Maximum deformation (mm)	43.02	37.30	27.42	21.98	19.90	30.60	23.22	17.10	15.12
	Residual plastic deformation (mm)	41.03	33.02	23.10	17.43	15.39	25.94	18.54	13.14	11.48
	Proportion of deformation that is resilient (%)	4.63	11.47	15.75	20.70	22.66	15.23	20.16	23.16	24.07